Knockout of Sporadic Creutzfeldt-Jakob Disease Risk Gene *Stx6* in Mice Extends Prion Disease Incubation Time

Emma Jones[a,1], Elizabeth Hill[a,1], Jacqueline Linehan[a], Tamsin Nazari[a], Adam Caulder[b], Gemma F Codner[b], Marie Hutchison[b], Matthew Mackenzie[b], Michael Wiggins De Oliveira[a], Huda Al-Doujaily[a], Malin Sandberg[a], Emmanuelle Viré[a], Thomas J Cunningham[a], Emmanuel A Asante[a,2], Sebastian Brandner[c], John Collinge[a], Simon Mead[a,3]

[a]Medical Research Council Prion Unit at University College London (UCL), UCL Institute of Prion Diseases, London W1W 7FF, United Kingdom

[b]Mary Lyon Centre at MRC Harwell, Harwell Campus, Oxfordshire OX11 0RD, UK

[c]Division of Neuropathology and Department of Neurodegenerative Disease, UCL Queen Square Institute of Neurology, Queen Square, London, WC1N 3BG, UK.

[1]These authors contributed equally to this work

[2]Present address: AsanSka University College of Design and Technology, P.O. Box VV 179, Oyibi, Ghana

[3]To whom correspondence may be addressed. Email: s.mead@prion.ucl.ac.uk

Abstract

Sporadic Creutzfeldt-Jakob disease (sCJD) is the most common human prion disease, which occurs when the cellular prion protein (PrP^C) spontaneously misfolds into disease-associated forms, culminating in fatal neurodegeneration. In a genome-wide association study of sCJD we recently identified risk variants in and around the gene *STX6*, with evidence to suggest a causal increase of *STX6* expression in disease-relevant brain regions. *STX6* encodes syntaxin-6, a SNARE protein primarily involved in early endosome to *trans*-Golgi network retrograde transport. Here we investigated a causal role of *Stx6* expression in mouse prion disease through a classical prion transmission study assessing the impact of homozygous and heterozygous syntaxin-6 knockout on disease incubation time and prion-related neuropathology. Homozygous ($Stx6^{-/-}$) and heterozygous ($Stx6^{+/-}$) knockout of *Stx6* expression extended survival by 12 days following inoculation with RML prions relative to wildtype controls. Similarly, in $Stx6^{-/-}$ mice, disease incubation time following inoculation with ME7 prions was extended by 12 days. Histopathological analysis revealed a modest increase in astrogliosis in ME7-inoculated $Stx6^{-/-}$ animals and a variable effect of *Stx6* expression on microglia activation, however no differences in neuronal loss, spongiform change or PrP deposition were observed at endpoint. Importantly, $Stx6^{-/-}$ mice are viable and fertile with no gross impairments on a range of neurological, biochemical, histological and skeletal structure tests. Our results provide confirmatory evidence for a pathological role of *Stx6* expression in prion disease and support further exploration of syntaxin-6 lowering as a potential therapeutic strategy.

Significance Statement

Sporadic Creutzfeldt-Jakob disease (sCJD), the most common human prion disease, is an invariably fatal disease with no disease-modifying treatments. The identification of *STX6* as a proposed risk gene for sCJD motivated the generation of a new mouse knockout model, in which we found no grossly deleterious phenotypes. A transmission study in *Stx6*$^{-/-}$, *Stx6*$^{+/-}$ and *Stx6*$^{+/+}$ mice showed a statistically significant prolongation in survival with two prion strains, providing evidence for a causal link of *Stx6* expression to prion disease pathogenesis. Syntaxin-6 appears to have pleiotropic risk effects across multiple neurodegenerative diseases including progressive supranuclear palsy and Alzheimer's disease. Thus, this work supports further exploration of *STX6* as a potential therapeutic target across multiple neurodegenerative diseases.

Introduction

Prion diseases are transmissible neurodegenerative conditions of humans and animals with no effective treatments. The infectious agent of prion diseases, or prion, is thought to comprise of assemblies of host prion protein in a parallel in register beta sheet conformation[1,2]. Sporadic Creutzfeldt-Jakob disease (sCJD), the most common human prion disease, is invariably and typically rapidly fatal. sCJD is thought to result from the spontaneous formation of prions in the body by misfolding of the host-encoded prion protein (PrP^C), triggering a self-perpetuating cycle whereby prions induce further PrP^C misfolding. Variation in the *PRNP* gene encoding PrP^C is a key genetic determinant of sCJD risk and phenotype, however there is now robust evidence for two non-*PRNP* genetic risk factors identified through a genome wide association study. These studies identified a genetic region including *STX6* as a novel risk locus in human sCJD[3]. Interestingly the *STX6* locus has also been implicated in other neurodegenerative diseases, with the same genetic variants being associated with progressive supranuclear palsy (PSP)[4,5] and increased syntaxin-6 protein expression being causally associated with Alzheimer's disease (AD)[6,7], indicating this protein may play a pleiotropic role in neurodegeneration.

STX6 encodes syntaxin-6, a member of the SNARE (soluble N-ethylmaleimide-sensitive factor attachment protein receptor) protein family, which are involved in the final step of membrane fusion during vesicle transport. Syntaxin-6 has been shown to be primarily involved in vesicle fusion during retrograde transport between early endosomes and the *trans*-Golgi network[8,9]. Analysis of expression quantitative trait loci (eQTLs) at this site identified *cis*-acting variants which increase *STX6* expression in disease-relevant brain regions, particularly the putamen and caudate nuclei, which are commonly found to be abnormal in diagnostic MRI brain studies in sCJD[10]. These and other gene prioritisation analyses identify *STX6* as the causal gene driving the increased sCJD risk at this locus.

Experimental inoculation of mice with prions faithfully recapitulates the neuropathological hallmarks seen in human prion diseases, notably the propagation and deposition of PrP aggregates, spongiform degeneration, neuronal loss and widespread glial cell and immune activation[11,12]. Furthermore, it has been long recognised that prions exist as conformationally distinct strains[13], which alter the disease progression and pathology in mice in a similar

manner to human diseases. Prion strains RML and ME7 have been developed, whereby prions originally derived from sheep and goat scrapie respectively have been serially passaged in mice resulting in adapted prions with high attack rates and well-defined incubation times in a laboratory setting[11,14]. Mouse bioassay has been routinely used to measure prion infectivity[15,16], as well as to further understand disease modifiers in a mammalian biological system[17,18]. In a standard experiment, the time from inoculation to prion disease diagnosis (termed "incubation time") is the defining endpoint.

To explore a role for *Stx6* expression in prion disease pathogenesis, we conducted a classical prion transmission study in a newly developed mouse model which has a genetic reduction in *Stx6* expression. We show that knockout of syntaxin-6 does not result in a deleterious phenotype and extended prion disease incubation time by 12 days following inoculation with RML or ME7 mouse-adapted scrapie prions, representing an 8% and 7% increase in survival relative to wildtype controls respectively. *Stx6*$^{+/-}$ mice showed an 8% prolongation of incubation time following RML inoculation, although no extension in survival was seen with ME7-inoculated *Stx6*$^{+/-}$ animals. No differences in neuronal loss, spongiform change or PrP deposition were seen between the genotypes, however a variable effect of *Stx6* expression on gliosis was observed at endpoint. This work provides complimentary evidence that altered expression of *Stx6* modifies prion disease pathogenesis and supports the further exploration of syntaxin-6 as a therapeutic target in neurodegenerative diseases.

Results

Generation of *Stx6* knockout C57BL/6N mice

We generated mice with homozygous deletion of *Stx6* (*Stx6*$^{-/-}$) on the C57BL/6N background as part of the International Mouse Phenotyping Consortium[19] (IMPC) via CRISPR/Cas9-mediated deletion of 1808 nucleotides spanning two critical exons (exons 6 and 7 of transcripts *Stx6-201* and *Stx6-209* as depicted in **Figure 1A**, present within all protein coding isoforms) replaced by an 8 nucleotide insertion, generating a premature stop codon. Quantitative immunoblotting of whole brain homogenates demonstrated the loss of the primary protein product at ~32 kDa in mice with homozygous deletion of *Stx6*, whilst heterozygous mice (*Stx6*$^{+/-}$) expressed ~50% of the protein compared to wildtype animals (*Stx6*$^{+/+}$) (*Stx6*$^{-/-}$: 0.0757% ± 0.0217 (mean ± SEM); *Stx6*$^{+/-}$: 55.9% ± 0.0436) (**Figure 1B-C**). This was also seen with an N-terminal syntaxin-6 antibody (**Supplementary Figure 1**). Reduced expression of PrP^{C} has previously been shown to extend incubation time in mice[20]. Therefore to determine any differences associated with *Stx6* expression, brain PrP^{C} levels were assessed by ELISA. This analysis did not reveal any differences in PrP^{C} expression with *Stx6* genotype (*Stx6*$^{+/+}$: 6115 ± 838.3 RFU (mean ± SEM); *Stx6*$^{+/-}$: 5784 ± 1100 RFU; *Stx6*$^{-/-}$: 5834 ± 153 RFU) (**Figure 1D**).

Stx6$^{-/-}$ mice are physiologically normal

To determine any gross changes in organ morphology associated with altered *Stx6* expression, immunohistochemical analysis was performed on liver, pancreas, kidney, skeletal muscle and adipose tissue dissected from 4-5 adult mice (4 x *Stx6*$^{-/-}$, 5 x *Stx6*$^{+/-}$, 5 x *Stx6*$^{+/+}$, see Supplementary Materials and Methods). As shown in **Figure 2**, there were no differences in the appearance and architecture between any tissue from *Stx6*$^{-/-}$, *Stx6*$^{+/-}$ and *Stx6*$^{+/+}$ animals aside from moderate liver steatosis in one *Stx6* null animal, however as this was only found in one animal it is unlikely to be related to the loss of *Stx6* expression (**Supplementary Figure 2**). Furthermore, analysis of skeletal structure by computed tomography (CT) scanning did not reveal any obvious differences in bone or skeleton architecture between genotypes (**Supplementary Figure 3**).

Upon generation, *Stx6*$^{-/-}$ mice were subject to the standard IMPC phenotyping program at MRC Harwell[21] (www.mousephenotype.org). This analysis suggested alterations in some

blood clinical chemistry parameters including increased blood urea nitrogen in early adult females and increased circulating alkaline phosphatase in early adult males, but these findings were not replicated in an independent sample (P > 0.01) (**Supplementary Table 1**, **Supplementary Figure 4**). The lack of replication or significance of these phenotypes in other sexes or life stages indicates these perturbations are not generalisable. Mice were examined on a range of behavioural and motor tasks, including nest building, rotarod, grip strength, pellets burrowed and weight of food consumed, with *Stx6*$^{-/-}$ and *Stx6*$^{+/-}$ (n = 5 per group) broadly comparable with wild-type animals (the study was not powered to detect subtle differences in behaviours). Overall, reduction in *Stx6* expression does not lead to any detectable deleterious phenotype in these animals.

Knockout of *Stx6* extends incubation times in mice infected with two mouse-adapted prion strains

To determine the effect of *Stx6* expression on survival and incubation time of prion disease, *Stx6*$^{-/-}$, *Stx6*$^{+/-}$ and *Stx6*$^{+/+}$ female mice were inoculated intracerebrally with two mouse-adapted scrapie prion strains, RML and ME7, or PBS as a negative control. A log-rank test of the association of disease incubation time with *Stx6* genotype showed a significant relationship in both RML (P = 0.0049, **Figure 3A**) and ME7 (P < 0.0001, **Figure 3C**) inoculated animals, demonstrating *Stx6* expression modulates survival time of prion disease with both prion strains.

To quantify these effects and define associations with specific genotypes, a secondary analysis was performed looking at the differences between partial and complete genetic reduction in *Stx6* expression for each strain. Following inoculation with RML prions, incubation time in *Stx6*$^{-/-}$ and *Stx6*$^{+/-}$ mice was extended by 12 days relative to wildtype animals (*Stx6*$^{+/+}$ = 147 days [144 – 161] (median [95% confidence interval]), *Stx6*$^{+/-}$ = 159 days [154 – 168], *Stx6*$^{-/-}$ = 159 days [156 – 160]) (**Figure 3A**). Furthermore, as a number of animals were censored in this analysis due to death prior to fulfilling the full scrapie sickness diagnostic criteria (especially for ME7 inoculated animals; see Supplementary Materials and Methods and **Supplementary Table 2**), the time from inoculation until onset of the first scrapie symptom was analysed (previously used as an alternative measure of incubation time[22]). There was no significant association of *Stx6* genotype with incubation time by this measure following RML inoculation (P = 0.14, **Figure 3B**), although there was still a modest increase in survival in *Stx6*$^{-/-}$ animals

compared to *Stx6*$^{+/+}$ (*Stx6*$^{+/+}$ = 133 days [127 – 139] vs *Stx6*$^{-/-}$ = 138 days [133 – 141]; *Stx6*$^{+/-}$ = 132 days [129 – 141]). Although this analysis allows for more representative inclusion of animals who were succumbing to the disease, identification of the first neurological symptom is typically a more variable assessment which likely underpins the differences between these two analyses.

In ME7-inoculated animals incubation time was also extended by 12 days with complete loss of *Stx6* compared to wildtype animals (*Stx6*$^{+/+}$ = 162 days [161 – 168]) vs *Stx6*$^{-/-}$ = 174 days [174 – NA], **Figure 3C**), however there was no increase seen with heterozygous *Stx6* expression with this strain (*Stx6*$^{+/-}$: 158 days [155 – 160]). In the analysis of time until onset of first neurological symptom, there was still a significant association of *Stx6* genotype ($P < 0.0001$, **Figure 3D**) with a 7-day increase in *Stx6*$^{-/-}$ mice compared to *Stx6*$^{+/+}$ animals (*Stx6*$^{+/+}$ = 147 days [146 – 150] vs *Stx6*$^{-/-}$ = 154 days [153 – 160]). Again however there was no effect of partial *Stx6* expression on this strain (*Stx6*$^{+/-}$ = 146 days [140 – 151]).

The independent observations of extended incubation time in *Stx6* knockout animals with two distinct prion strains supports a general pathological role of expression of this gene in prion disease progression. *Stx6* may select for propagation of distinct strains. To assess this, we performed western blotting on end stage brain homogenates which demonstrated no change of PrP scrapie types with modified *Stx6* expression in either RML or ME7 inoculated animals as expected (**Supplementary Figure 5**).

Neuropathological features and *Stx6* expression

Prion disease is typically characterised by histological features of spongiform vacuolation, neuronal loss and astrocyte proliferation[23], along with deposition of PrP aggregates in the brain and a strong microglia response, which can be identified upon brain biopsy in patients, or on post-mortem histopathological analysis of the brain in patients and animals[24]. Immunohistochemical staining with an anti-PrP antibody detected PrP deposits at the end-stage of the disease following intracerebral inoculation with RML and ME7 prions in all animals (7-10 mice analysed per group, see Supplementary Materials and Methods) (**Figure 4**). With both strains, disease-associated PrP can be detected with a diffuse staining pattern in grey matter areas. In ME7-inoculated animals there was additional widespread deposition

of micro-plaques as previously described[24]. Knockout of *Stx6* did not cause detectable deposition of disease-associated PrP in PBS-inoculated controls as expected. At this resolution and time-point there was no difference evident in appearance, extent or localisation of PrP aggregates between *Stx6* genotypes.

To determine whether there were any differences in spongiform vacuolation with *Stx6* expression at endpoint, haematoxylin and eosin (H&E) staining was used to identify morphological changes in the tissue. This analysis revealed the presence of distinct small, round vacuoles within the neuropil in multiple brain regions including the striatum, cortex and midbrain in prion-inoculated animals, reflecting the expected spongiform change associated with prion disease (**Figure 5**). This analysis also showed the typical neuronal loss within the hippocampus following ME7 inoculation. No changes were identified in controls demonstrating knockout of *Stx6* alone does not induce pathological changes. Taken together, these results provide further support for maintenance in prion strain type in mice with genetic reduction of syntaxin-6, with no clear differences in PrP deposition patterns and spongiform vacuolation between genotypes.

Possible increased inflammatory response with reduced *Stx6* expression

As widespread activation and proliferation of both astrocytes and microglia is a hallmark of both human and animal prion disease, and progresses with disease duration, immunohistochemical staining was performed to detect activated astrocytes and microglial cells and to quantify any modulatory effects *Stx6* expression may have on neuroinflammatory phenotypes in prion disease. Furthermore, control animals were analysed to determine if *Stx6* knockout alone causes any inflammatory phenotypes.

Immunohistochemical staining of reactive astrocytes with an anti-GFAP antibody confirmed the expected widespread astrocyte proliferation, with particular intensity in the thalamus and hippocampus as previously described in prion disease[25] (**Figure 6A**). Quantification of mean percentage area shows >70% immunoreactivity in brain tissue under all prion-inoculated conditions (ME7: *Stx6*$^{-/-}$ = 82.3% ± 0.820 (mean ± SEM), *Stx6*$^{+/-}$ = 71.7% ± 0.870, *Stx6*$^{+/+}$ = 70.7% ± 2.15; RML: *Stx6*$^{-/-}$ = 79.2% ± 1.06, *Stx6*$^{+/-}$ = 82.6% ± 1.20, *Stx6*$^{+/+}$ = 78.6% ± 1.06) compared to ~40% in PBS-inoculated animals (PBS: *Stx6*$^{-/}$ = 42.4% ± 1.04, *Stx6*$^{+/-}$ = 44.3% ±

0.630, *Stx6*$^{+/+}$ = 43.7% ± 0.478) (**Figure 6C**). This highlighted a ~10% increase in astrocyte area in *Stx6*$^{-/-}$ mice inoculated with ME7 relative to both *Stx6*$^{+/-}$ (P_{adj} = 1.70 x 10^{-3}) and *Stx6*$^{+/+}$ animals (P_{adj} = 7.57 x 10^{-4}) after adjusting for age of death to take into account the later tissue collection for the *Stx6*$^{-/-}$ mice with extended survival. Of note, there was no significant association between age and GFAP area stained. This highlights a potential protective mechanism for reduced *Stx6* expression in prion diseases, for example if astrocytes are acting to maintain neuronal function.

Immunostaining with anti-Iba1 antibody to detect microgliosis demonstrated the expected visible microglia activation following inoculation with both RML and ME7 prions, occupying 25-30% of the whole brain area in all disease conditions (ME7: *Stx6*$^{-/-}$ = 25.3% ± 1.20, *Stx6*$^{+/-}$ = 28.1% ± 0.972, *Stx6*$^{+/+}$ = 24.8% ± 1.26; RML: *Stx6*$^{-/-}$ = 23.7% ± 1.03, *Stx6*$^{+/-}$ = 29.9% ± 1.06, *Stx6*$^{+/+}$ = 24.5% ± 0.899) compared to ~8% in control animals (PBS: *Stx6*$^{-/-}$ = 7.37% ± 1.33, *Stx6*$^{+/-}$ = 8.77% ± 0.525, *Stx6*$^{+/+}$ = 7.09% ± 0.700) (**Figure 6B, D**). Interestingly in all conditions *Stx6*$^{+/-}$ mice demonstrated a modestly higher proportion of microglia relative to both *Stx6*$^{+/+}$ and *Stx6*$^{-/-}$ mice, which was significant in RML inoculated animals after adjusting for different ages at death (P_{adj} = 4.07 x 10^{-3} and P_{adj} = 1.74 x 10^{-4} respectively).

Discussion

Extended Survival Times in *Stx6*$^{-/-}$ Mice Following Intracerebral Inoculation with RML and ME7 Mouse-Adapted Scrapie Prions.

Mouse models are a powerful method to assess the role of human risk genes as they are naturally susceptible to prion diseases, and prion-infected animals faithfully recapitulate many of the key aspects of human disease. Knockout of *Stx6* in C57BL/6N female mice prolonged mouse prion disease incubation time for both strains tested. Although the extension of 12 days is modest, this was expected considering the moderate effect sizes for typical risk alleles detected by GWAS (*STX6* odds ratio (OR) = 1.16)[3] and potential compensatory mechanisms associated with complete gene knockout. Whilst these were well-controlled experiments, it remains possible that modest changes in incubation time might have resulted from imbalance in unmeasured confounding factors. PrP^C levels were comparable between the genotypes suggesting a direct interaction of *Stx6* on *Prnp* expression was not the driving force behind the observation however we cannot exclude subtle effects on the expression or distribution of PrP^C and it remains possible, even likely, that *Stx6* modifying effects are exerted through altered trafficking of PrP^C or disease associated forms of the protein. Although we recently identified risk variants associated with sCJD at the *STX6* locus, proximity of risk SNPs to genes is suggestive but not sufficient to establish causality. Integration of GWAS variants with eQTL data provided evidence *STX6* expression is associated with disease risk. These mouse data are therefore in keeping with the hypothesis derived from GWAS discovery that increased *STX6* expression promotes prion disease pathogenesis. Importantly however, prion transmission studies model a form of acquired prion disease, raising the possibility that syntaxin-6 plays a role across different aetiologies of prion disease and across species.

Assessment of Prion-Related Phenotypes

No differences in neuronal loss and the extent or distribution of PrP pathology were noted between *Stx6*$^{+/+}$, *Stx6*$^{+/-}$ and *Stx6*$^{-/-}$ mice. This indicates that *Stx6* expression does not alter disease progression through a gross effect on disease pathology. However, it should be noted that this was assessed in endpoint animals where neuropathology was severe and

quantification of these was not possible due to processing artefacts, which may have masked more subtle differences. Furthermore, ages of mice were not matched, as *Stx6*$^{-/-}$ mice generally survived longer than the wild-type controls. In contrast, quantitative comparisons of gliosis between the genotypes revealed some subtle differences. Interestingly a ~10% increase in astrocyte count was seen in ME7-infected *Stx6*$^{-/-}$ mice and a ~5% increase in microglia count was seen in RML-infected *Stx6*$^{+/-}$ mice relative to *Stx6*$^{+/+}$ animals. Furthermore, in all conditions *Stx6*$^{+/-}$ mice demonstrated a modestly higher proportion of microglia relative to both *Stx6*$^{+/+}$ and *Stx6*$^{-/-}$ mice, which may reflect a dose-dependent effect of *Stx6* expression on microglia function. To exclude the possibility that these differences were driven by different ages of animals at endpoint, we included age at death in days as a covariate in the regression analysis with no significant effect found. Considering syntaxin-6 itself has been proposed as a particularly promiscuous SNARE protein with a multitude of cell-type specific functions, it is certainly plausible that the pathological role of syntaxin-6 is mediated through non-neuronal cell types. Taken together, these results suggest a possible role for syntaxin-6 in the supporting cells of the brain, fitting with the increasing acceptance that prion disease pathobiology is driven by the interaction of multiple cell types and non-cell autonomous mechanisms[26,27].

Targeting Syntaxin-6 as a Therapeutic Strategy

Human genetic evidence increasingly supports successful drug development programmes[28]. The identification and proposal of *STX6* as a risk gene through GWAS therefore provokes research about therapeutic potential, which is in part supported by this *in vivo* study. Importantly for therapeutic utility, *Stx6*$^{-/-}$ mice are viable and fertile with no gross neurological or physiological impairments. Although the IMPC have recorded some potential metabolic and behavioural alterations in *Stx6*$^{-/-}$ mice, these were not reproducible across life stages and gender, and were not replicated in our mouse cohort. Further work involves determining the efficacy of targeting *Stx6* during the disease course. The pleiotropic role of syntaxin-6 across multiple neurodegenerative diseases, including PSP and AD, raises the potential that *STX6*-targeting therapies could have wider applicability to other neurodegenerative diseases.

Potential Mechanistic Roles of Syntaxin-6 in Prion Disease Pathology

As a key intracellular trafficking protein, it is plausible that modified syntaxin-6 function alters the transport of PrP^C and/or disease-associated prions throughout the cell. Considering syntaxin-6 is thought to be involved in the recycling of proteins from endosomes[29,30], knockout of *Stx6* could conceivably result in reduced transport of disease-associated PrP away from these structures and thus increased degradation in the lysosomal pathway, with obvious benefits for prion load. Alternatively a similar hypothesis could be proposed for transport of toxic species in prion diseases. Recent work indicated a role of syntaxin-6 in the kinetic formation of toxic PrP structures *in vitro*, however whether a direct protein interaction occurs *in vivo* is unclear[31]. Finally, it is plausible the effect of modified syntaxin-6 function has more widespread implications for cellular function, which may indirectly affect prion disease biology.

Materials and Methods

Stx6$^{+/-}$ mice (C57BL/6NTac-*Stx6*$^{em1(IMPC)H}$/H) were generated and crossbred to establish homozygous *Stx6*$^{-/-}$ and *Stx6*$^{+/+}$ lines. *Stx6*$^{+/-}$ litters were subsequently obtained through crossbreeding of these two lines. For the prion transmission study, anaesthetised female *Stx6*$^{-/-}$, *Stx6*$^{+/-}$ and *Stx6*$^{+/+}$ mice were inoculated intracerebrally in the right parietal lobe with 30 µl 1% (w/v) C57BL/6 mouse-adapted RML or ME7 prion-infected brain homogenate (n = 20 per group) or PBS (n = 5 per group) at 6-8 weeks of age as previously described[32]. Mice were monitored daily and culled following diagnosis with scrapie sickness according to established criteria or identification of distinct health concerns[32]. Incubation time was defined as the number of days from inoculation until definite scrapie diagnosis[32]; disease-free incubation time was defined as the number of days from inoculation to first scrapie-associated neurological symptom. Immunohistochemistry was performed on tissue fixed in 10% buffered formal saline, processed, paraffin wax embedded and serial sections of 5 µm nominal thickness were taken as previously described with modifications[33]. Detailed material and methods for genotyping, Western blotting, ELISA, immunohistochemistry and phenotyping assays are provided in Appendix, Supplementary Materials and Methods.

Acknowledgments

We thank Florin Pintilii, Helena Costa and Fabio Argentina for further technical assistance with immunohistochemistry, Dr Jonathan Wadsworth for training support, the staff of the MRC Prion Unit at UCL Biological Services Facility for animal husbandry and experimental assistance, Dr Tammy Kalber for assistance with CT scanning and Shyma Hamdan for assistance with animal genotyping. This work was funded by the UK Medical Research Council. Simon Mead and John Collinge are National Institute for Health Research Senior Investigators.

References

1 Kraus, A. *et al.* High-resolution structure and strain comparison of infectious mammalian prions. *Mol Cell* **81**, 4540-4551.e4546, doi:10.1016/j.molcel.2021.08.011 (2021).

2 Manka, S. W. *et al.* 2.7 Å cryo-EM structure of ex vivo RML prion fibrils. *Nature Communications* **13**, 4004, doi:10.1038/s41467-022-30457-7 (2022).

3 Jones, E. *et al.* Identification of novel risk loci and causal insights for sporadic Creutzfeldt-Jakob disease: a genome-wide association study. *The Lancet. Neurology* **19**, 840-848, doi:10.1016/s1474-4422(20)30273-8 (2020).

4 Höglinger, G. U. *et al.* Identification of common variants influencing risk of the tauopathy progressive supranuclear palsy. *Nature Genetics* **43**, 699-705, doi:10.1038/ng.859 (2011).

5 Ferrari, R. *et al.* Assessment of common variability and expression quantitative trait loci for genome-wide associations for progressive supranuclear palsy. *Neurobiology of Aging* **35**, 1514.e1511-1514.e1511, doi:10.1016/j.neurobiolaging.2014.01.010 (2014).

6 Wingo, A. P. *et al.* Integrating human brain proteomes with genome-wide association data implicates new proteins in Alzheimer's disease pathogenesis. *Nature Genetics* **53**, 143-146, doi:10.1038/s41588-020-00773-z (2021).

7 Yu, L. *et al.* Neuropathologic Correlates of Human Cortical Proteins in Alzheimer Disease and Related Dementias. *Neurology*, doi:10.1212/wnl.0000000000013252 (2021).

8 Bock, J. B., Lin, R. C. & Scheller, R. H. A new syntaxin family member implicated in targeting of intracellular transport vesicles. *The Journal of biological chemistry* **271**, 17961-17965, doi:10.1074/jbc.271.30.17961 (1996).

9 Bock, J. B., Klumperman, J., Davanger, S. & Scheller, R. H. Syntaxin 6 functions in trans-Golgi network vesicle trafficking. *Molecular biology of the cell* **8**, 1261-1271, doi:10.1091/mbc.8.7.1261 (1997).

10 Zerr, I. *et al.* Updated clinical diagnostic criteria for sporadic Creutzfeldt-Jakob disease. *Brain* **132**, 2659-2668, doi:10.1093/brain/awp191 (2009).

11 Chandler, R. L. Encephalopathy in mice produced by inoculation with scrapie brain material. *Lancet* **1**, 1378-1379, doi:10.1016/s0140-6736(61)92008-6 (1961).

12 Aguzzi, A., Barres, B. A. & Bennett, M. L. Microglia: scapegoat, saboteur, or something else? *Science (New York, N.Y.)* **339**, 156-161, doi:10.1126/science.1227901 (2013).

13 Fraser, H. & Dickinson, A. G. Scrapie in mice. Agent-strain differences in the distribution and intensity of grey matter vacuolation. *J Comp Pathol* **83**, 29-40, doi:10.1016/0021-9975(73)90024-8 (1973).

14 Zlotnik, I. & Rennie, J. C. Further observations on the experimental transmission of scrapie from sheep and goats to laboratory mice. *J Comp Pathol* **73**, 150-162, doi:10.1016/s0368-1742(63)80018-1 (1963).

15 Sandberg, M. K., Al-Doujaily, H., Sharps, B., Clarke, A. R. & Collinge, J. Prion propagation and toxicity in vivo occur in two distinct mechanistic phases. *Nature* **470**, 540-542, doi:10.1038/nature09768 (2011).

16 Sandberg, M. K. *et al.* Prion neuropathology follows the accumulation of alternate prion protein isoforms after infective titre has peaked. *Nature Communications* **5**, 4347, doi:10.1038/ncomms5347 (2014).

17 Akhtar, S. *et al.* Sod1 deficiency reduces incubation time in mouse models of prion disease. *PloS one* **8**, e54454, doi:10.1371/journal.pone.0054454 (2013).

18 Grizenkova, J. *et al.* Overexpression of the Hspa13 (Stch) gene reduces prion disease incubation time in mice. *Proceedings of the National Academy of Sciences of the United States of America* **109**, 13722-13727, doi:10.1073/pnas.1208917109 (2012).

19 Groza, T. *et al.* The International Mouse Phenotyping Consortium: comprehensive knockout phenotyping underpinning the study of human disease. *Nucleic Acids Research*, gkac972, doi:10.1093/nar/gkac972 (2022).

20 Büeler, H. *et al.* Mice devoid of PrP are resistant to scrapie. *Cell* **73**, 1339-1347, doi:10.1016/0092-8674(93)90360-3 (1993).
21 Dickinson, M. E. *et al.* High-throughput discovery of novel developmental phenotypes. *Nature* **537**, 508-514, doi:10.1038/nature19356 (2016).
22 Carlson, G. A. *et al.* Linkage of prion protein and scrapie incubation time genes. *Cell* **46**, 503-511, doi:10.1016/0092-8674(86)90875-5 (1986).
23 Budka, H. Neuropathology of prion diseases. *British Medical Bulletin* **66**, 121-130, doi:10.1093/bmb/66.1.121 (2003).
24 Wenborn, A. *et al.* A novel and rapid method for obtaining high titre intact prion strains from mammalian brain. *Scientific Reports* **5**, 10062, doi:10.1038/srep10062 (2015).
25 Makarava, N., Chang, J. C., Kushwaha, R. & Baskakov, I. V. Region-Specific Response of Astrocytes to Prion Infection. *Front Neurosci* **13**, 1048, doi:10.3389/fnins.2019.01048 (2019).
26 Tahir, W. *et al.* An astrocyte cell line that differentially propagates murine prions. *The Journal of biological chemistry* **295**, 11572-11583, doi:10.1074/jbc.RA120.012596 (2020).
27 Smith, H. L. *et al.* Astrocyte Unfolded Protein Response Induces a Specific Reactivity State that Causes Non-Cell-Autonomous Neuronal Degeneration. *Neuron* **105**, 855-866.e855, doi:10.1016/j.neuron.2019.12.014 (2020).
28 Ochoa, D. *et al.* Human genetics evidence supports two-thirds of the 2021 FDA-approved drugs. *Nat Rev Drug Discov*, doi:10.1038/d41573-022-00120-3 (2022).
29 Mallard, F. *et al.* Early/recycling endosomes-to-TGN transport involves two SNARE complexes and a Rab6 isoform. *J Cell Biol* **156**, 653-664, doi:10.1083/jcb.200110081 (2002).
30 Chao, D. S. *et al.* SNARE membrane trafficking dynamics in vivo. *J Cell Biol* **144**, 869-881, doi:10.1083/jcb.144.5.869 (1999).
31 Sangar, D., Jack, K., Batchelor, M., Mistry, B. & Bieschke, J. Syntaxin 6 delays prion protein fibril formation and prolongs presence of toxic aggregation intermediates. *bioRxiv*, 2022.2008.2025.505283, doi:10.1101/2022.08.25.505283 (2022).
32 O'Shea, M. *et al.* Investigation of Mcp1 as a Quantitative Trait Gene for Prion Disease Incubation Time in Mouse. *Genetics* **180**, 559-566, doi:10.1534/genetics.108.090894 %J Genetics (2008).
33 Wadsworth, J. D. F. *et al.* Humanised transgenic mice are resistant to chronic wasting disease prions from Norwegian reindeer and moose. *J Infect Dis*, doi:10.1093/infdis/jiab033 (2021).
34 Akhtar, S., Wenborn, A., Brandner, S., Collinge, J. & Lloyd, S. E. Sex Effects in Mouse Prion Disease Incubation Time. *PloS one* **6**, e28741, doi:10.1371/journal.pone.0028741 (2011).
35 Wadsworth, J. D. F. *et al.* Methods for Molecular Diagnosis of Human Prion Disease. *Methods Mol Biol* **1658**, 311-346, doi:10.1007/978-1-4939-7244-9_22 (2017).

Figures

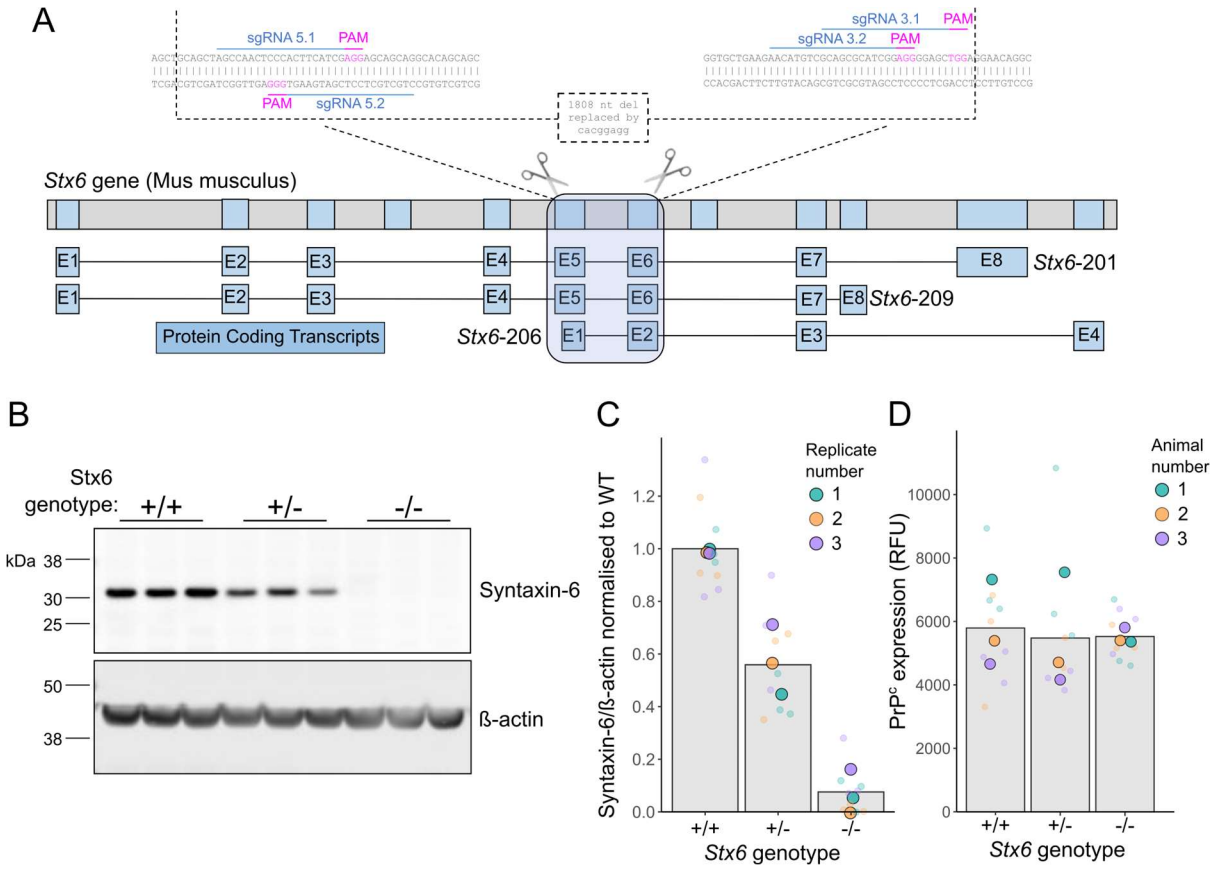

Figure 1: Development and validation of Stx6 knockout mice. (A) *Strategy for CRISPR/Cas9-mediated knockout of Stx6 in C57BL/6N mice. Four single guide RNAs (sgRNAs) targeting the DNA sequences in exons 5 and 6 of the two main Stx6 protein-coding transcripts (Stx6-201 and Stx6-209), also encompassing the N-terminal portion of the shorter Stx6-206 transcript, were selected for gene editing in zygotes. This resulted in an 1808 nucleotide (nt) deletion replaced by an 8 nt insertion. Top: Full Stx6 gene in the genome. Bottom: protein coding transcripts. Inset: CRISPR/Cas9 genome editing at Stx6 locus.* ***(B)*** *Representative quantitative immunoblots with anti-syntaxin 6 and anti-β actin antibodies of whole brain homogenates from* $Stx6^{+/-}$*,* $Stx6^{-/-}$ *and* $Stx6^{+/+}$ *mice and* ***(C)*** *quantification of syntaxin-6 intensity relative to β-actin normalised to* $Stx6^{+/+}$ *control demonstrates loss of primary ~32 kDa protein isoform in* $Stx6^{-/-}$ *mice (0.0757% ± 0.0217 (mean ± SEM)) with ~50% expression (55.9% ± 0.0436) in* $Stx6^{+/-}$ *mice (n = 3 per group, n = 3 technical replicates).* ***(D)*** *Analysis of* PrP^{C} *expression in whole brain homogenates from* $Stx6^{-/-}$*,* $Stx6^{+/-}$ *and* $Stx6^{+/+}$ *early adult 9 week old mice by ELISA does not indicate any significant differences between lines (*$Stx6^{+/+}$*: 6115 ± 838.3 relative fluorescent units (RFU);* $Stx6^{+/-}$*: 5784 ± 1100 RFU;* $Stx6^{-/-}$*: 5834 ± 153 RFU) (one-way ANOVA on square root transformed data).*

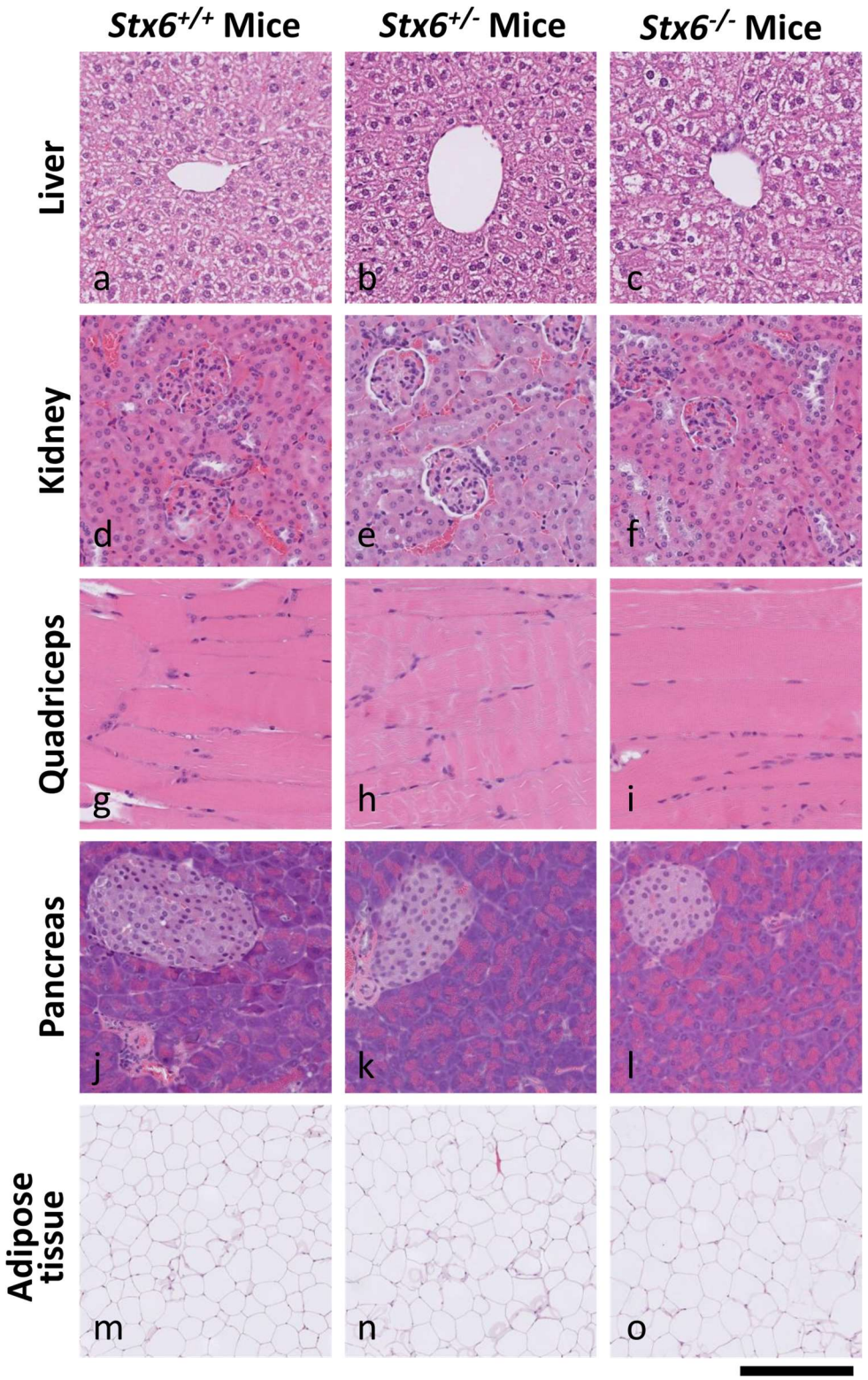

Figure 2: Multi-organ H&E staining shows expected tissue architecture and appearance in Stx6$^{-/-}$ and Stx6$^{+/-}$ mice which lack consistent tissue-intrinsic pathologies. *The following organs were harvested from Stx6$^{+/+}$ (n = 5), Stx6$^{+/-}$ (n = 5) and Stx6$^{-/-}$ (n = 4) female mice at 56-61 weeks of age: liver, pancreas, kidney, skeletal muscle and white adipose. These were formalin fixed, processed to paraffin and underwent H&E staining, revealing no consistent differences between genotypes. Scale bar corresponds to 120 µm (a-l), and 500 µm (m-o).*

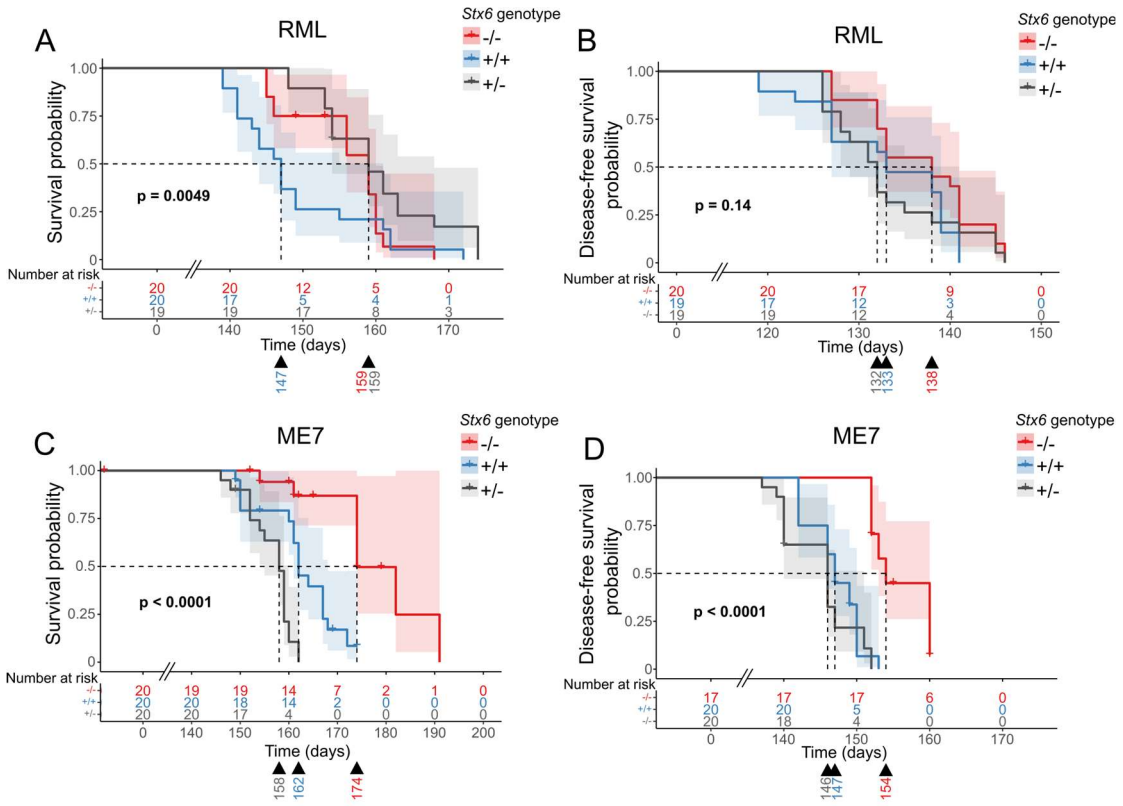

Figure 3: Extended survival times in Stx6$^{-/-}$ mice following intracerebral inoculation with RML and ME7 mouse-adapted scrapie prions. *(**A**-**D**) Kaplan meier curve of survival probability following intracerebral inoculation of Stx6$^{-/-}$ (red), Stx6$^{+/-}$ (grey) and Stx6$^{+/+}$ (blue) C57BL/6N mice (n = 20 per group) with 1% brain homogenate from (**A**,**B**) RML and (**C**,**D**) ME7 infected C57BL/6 mice. (**A**, **C**) Survival probability until animals were culled due to scrapie sickness shows a 12-day increase in median survival time for (**A**) both Stx6$^{-/-}$ and Stx6$^{+/-}$ mice following RML inoculation and (**C**) for Stx6$^{-/-}$ mice only following ME7 inoculation relative to Stx6$^{+/+}$ mice. (**B**,**D**) Disease-free survival probability (time until onset of the first scrapie symptom) (**B**) does not show a significant association with Stx6 genotype following RML-inoculation but a nominal 5-day increase in median incubation time in Stx6$^{-/-}$ mice compared to (**D**) a 7-day increase in Stx6$^{-/-}$ mice inoculated with ME7, relative to Stx6$^{+/+}$ mice. P-values indicate statistical associations with group determined using a log-rank test. Median incubation time shown below each plot. Crosses indicate censored animals.*

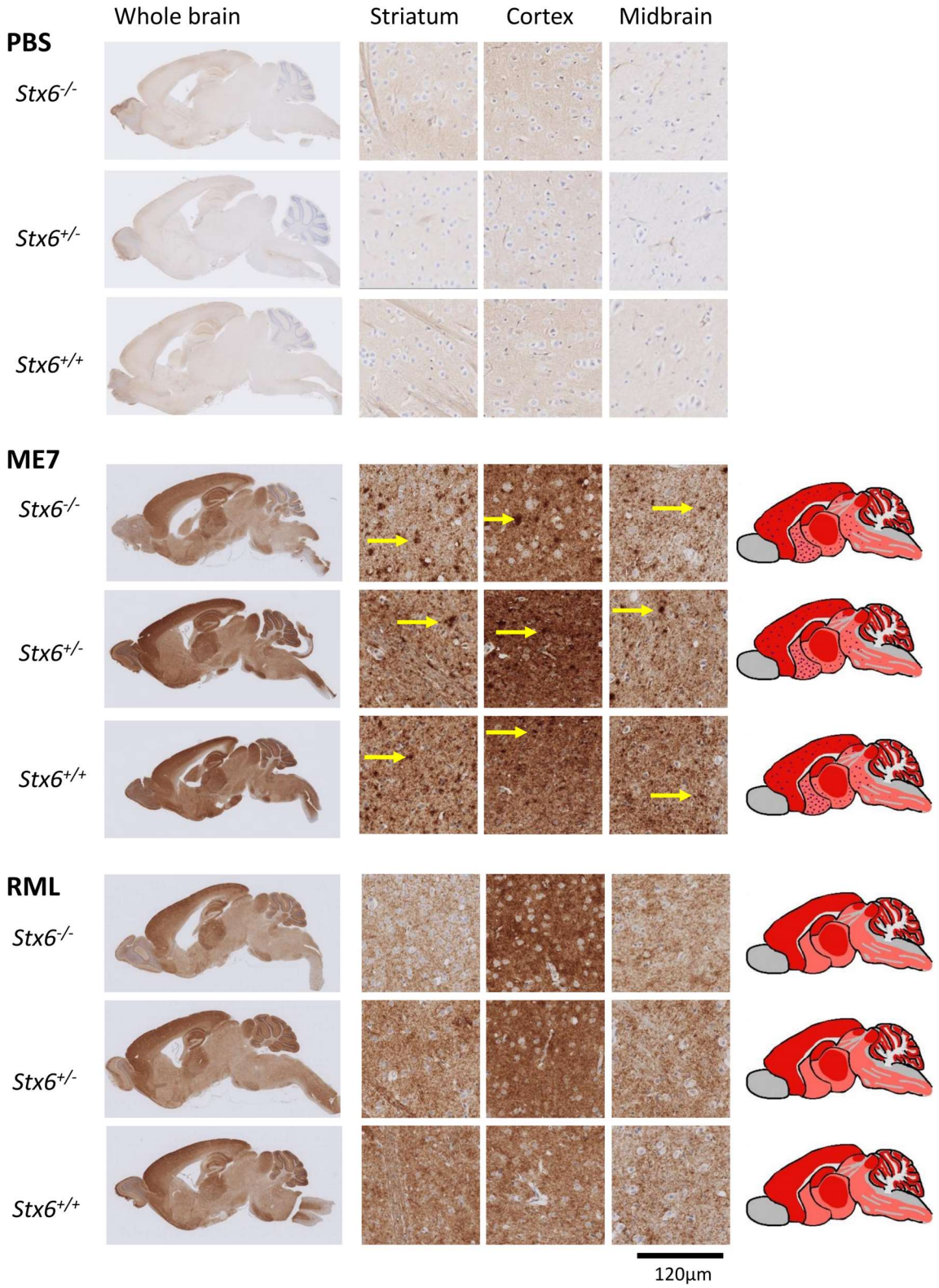

Figure 4: Knockout of Stx6 does not alter PrP deposition in prion infected mice. *Immunohistochemistry using anti-PrP antibody ICSM35 in whole brain (left) with schematic depiction of PrP deposition (pink shading: moderate PrP deposition; red shading: intense PrP deposition; red dots: PrP micro-plaques) or representative images from striatum, cortex and*

midbrain (middle) from Stx6$^{-/-}$, Stx6$^{+/-}$ and Stx6$^{+/+}$ mice inoculated with PBS (top) or ME7 (middle) and RML (bottom) mouse-adapted scrapie prions, shows expected PrP deposition in all prion-inoculated samples at end-point, with widespread diffuse staining for both strains and additional presence of micro-plaques with ME7 (yellow arrows). There was no evidence of spontaneous PrP deposition in control animals or gross difference evident between genotypes.

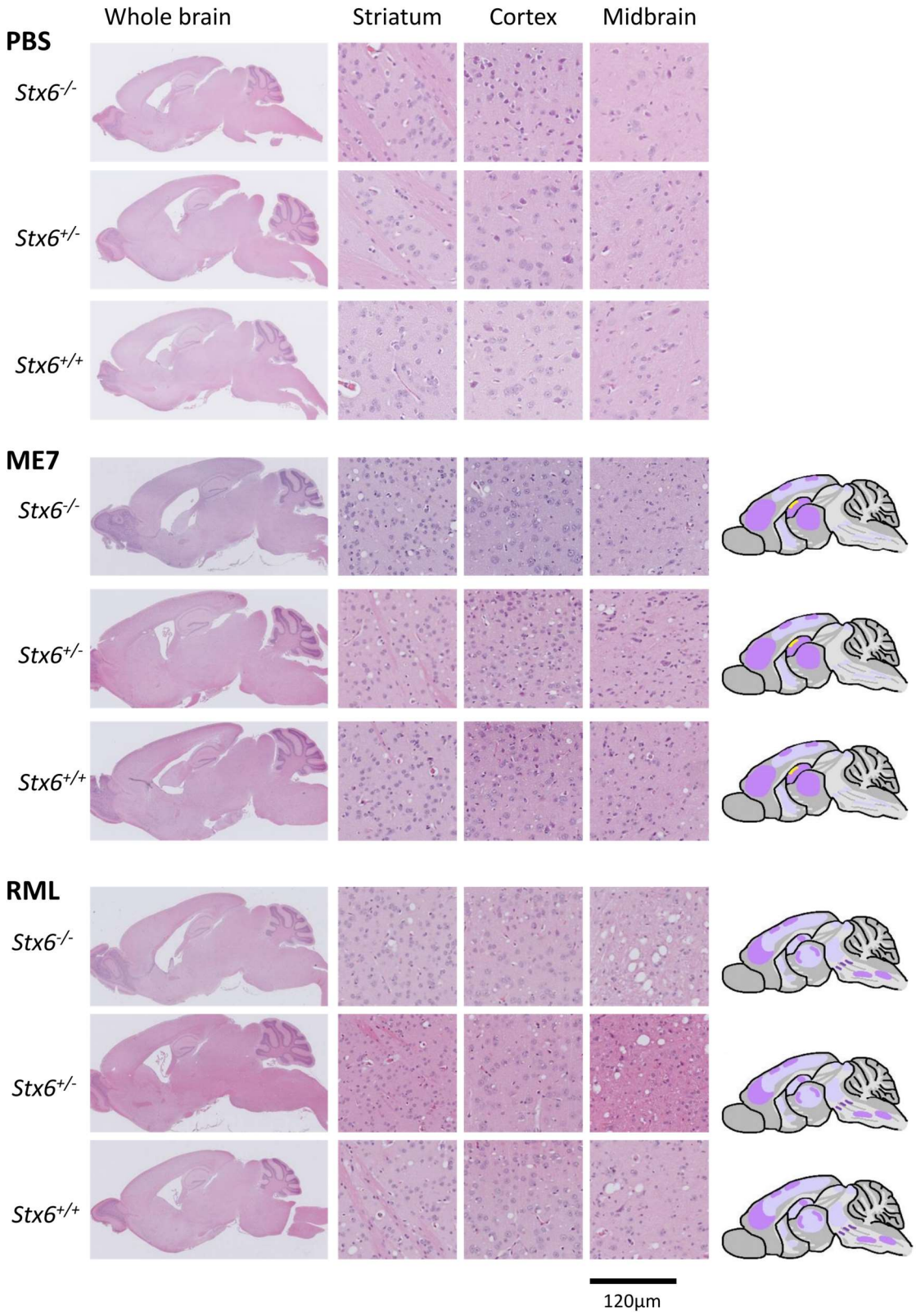

Figure 5: Neuronal loss and spongiform change were comparable in end-stage Stx6$^{-/-}$, Stx6$^{+/-}$ and Stx6$^{+/+}$ mice. *Haematoxylin and eosin (H&E) staining of whole brain (left) with schematic depiction of spongiosis (right; light purple shading: widely dispersed spongiosis; darker purple shading: intense focal spongiosis; yellow shading: neuronal loss) and representative images*

from striatum, cortex and midbrain (middle) from Stx6$^{-/-}$, Stx6$^{+/-}$ and Stx6$^{+/+}$ mice inoculated with PBS (top) or ME7 (middle) and RML (bottom) mouse-adapted scrapie prions shows expected spongiform pathology in all samples at end-point, including hippocampal neuronal loss with ME7, with no gross differences evident between genotypes. No neuropathology was evident in PBS-inoculated controls.

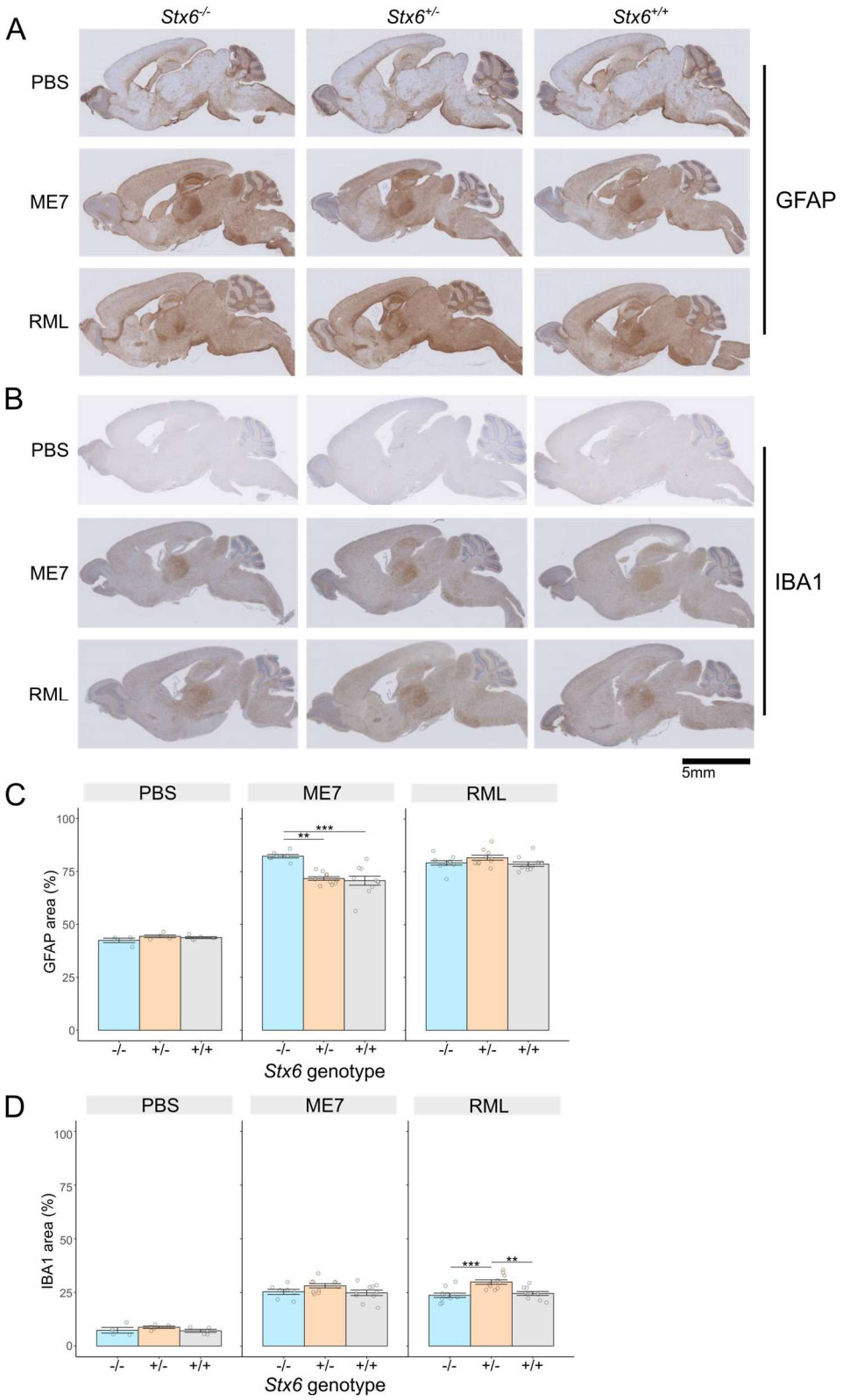

Figure 6: Variable effect of Stx6 genotype on neuroinflammation in prion disease. *(**A, B**) Example images of immunohistochemistry in Stx6$^{-/-}$, Stx6$^{+/-}$ and Stx6$^{+/+}$ mice inoculated PBS control or ME7 and RML mouse-adapted scrapie prions with (**A**) anti-GFAP antibody to measure reactive astrocytes and (**B**) anti-Iba1 antibody to measure microgliosis, shows expected neuroinflammation in prion-infected animals, including expected intense staining in*

*the thalamus with both antibodies and intense GFAP staining in the hippocampus. (**C**, **D**) Quantification of percentage area stained with (**C**) anti-GFAP and (**D**) anti-Iba1 antibody demonstrates a ~10% increase in astrocyte area in ME7-inoculated Stx6$^{-/-}$ animals and a ~5% increase in microglia area in Stx6$^{+/-}$ mice in RML-inoculated animals (linear regression model adjusted for age of death; ** $P < 0.01$, *** $P < 0.001$).*